23rd ABCM International Congress of Mechanical Engineering
December 6-11, 2015, Rio de Janeiro, RJ, Brazil

DESIGN AND APPLICATION OF A LOW COST HELMHOLTZ COILS FOR MAGNETOMETER CALIBRATION AND HIL SIMULATIONS

Daniel Strufaldi Batista
Francisco Granziera Jr
Gabriel Rezende Germanovix
Marcelo Carvalho Tosin
State University of Londrina, Rodovia Celso Garcia Cid Pr 445 Km 380, Londrina/PR, Brazil
daniel.strufaldi@gmail.com; granziera@uel.br; g.germanovix@gmail.com; mctosin@uel.br

Abstract. *This work presents the design and construction of a low cost three-axial Helmholtz coil developed to generate a uniform magnetic field. The coil was built using only non-magnetic materials and the design implemented was a rectangular Helmholtz coil formed by the junction of three pairs of single coils. It has approximately one cubic meter and it is capable of generating an 11 cm uniform cubic magnetic field around its center. The work presents concepts and theoretical fundaments involving Helmholtz theory, requirements and details of the low cost system developed. Results of the magnetic field obtained are presented and a discussion about the capability of the system is made. Finally the work also discuss two main applications in which this coil will be tested. One of the main application is to calibrate magnetic sensors, especially Micro-Electro-Mechanical Systems (MEMS) magnetometers. The system will also be used to simulate Earth's magnetic field for hardware-in-the-loop simulations, being capable of simulating the field that a satellite will be exposed during its flight.*

Keywords: *Helmholtz Coil, Magnetic Field, Magnetometer, Calibration, Hardware-in-the-loop*

1. INTRODUCTION

The Helmholtz coil is a tool designed by Hermann Ludwig Ferdinand von Helmholtz (1821-1894) which consists of two parallel coaxial circular coils. Due to the symmetry of its structure and the proximity between both coils it is possible to generate a uniform magnetic field in a small region around the center of the coils set. Applying a continuous current in the same direction on both pairs of windings generates a magnetic field which is proportional to the current intensity and to the number of windings.

Considering the rectangular coordinates, the Helmholtz coil is able to generate an uniform field in only one direction of the triad. In order to generate a field in any direction it is used three Helmholtz coils aligned in each of the axis **x, y, z** on the rectangular coordinate (orthogonal directions). This arrangement enables the generation of a cubic volume of uniform magnetic field, which critical to the calibration function of navigation equipment (Beravs *et al.*, 2014).

With the development of miniaturized sensors, a new range of applications emerged, from small personal devices such as smart phones and video games, to unmanned vehicles and spatial application such as nano- satellites, among others.

Magnetometers are one of these sensors often used. They can be used to build an electronic compass that can indicate the angle to the magnetic north with a precision better than $1°$. If associated with other type of sensors, such as accelerometers, then in non-accelerated applications it is possible to determine not only one angle, but the three angles (Euler angles) that completely represent the attitude, or rotation, of the body in relation to a frame reference.

Just like any sensors magnetometers are subject to errors. To work properly it is necessary to obtain the parameters of a calibration model that compensates most of the errors and distortions.

Most applications involving attitude uses orthogonal triads of magnetic sensors. Case this triad were perfect with all sensors perfectly identical and calibrated, its randomly rotation under the effect of a constant magnetic field, the simultaneous reading of all axis would form a trail of points on the surface of a sphere with constant radius.

Due to errors such as offsets, scale factor and misalignment between the axes those points does not generate a sphere but a rotated ellipsoid slightly distorted, which center is not at the origin.

The mathematical description of a sphere at the origin is simple and its necessary to know only its radious. On the contrary, the quadratic term representing this measured ellipsoid is not trivial and it is necessary at least nine parameters to recreate it. These parameters are three offsets and three scale factor (one for each axis) and the three possible angles between the triads.

Foster and Elkaim (2008) proposes a way to make the estimation of this ellipsoid using simulated data, Granziera Jr *et al.* (2011a) apply this algorithm to real sensor data and the results were promising, but certain limitations made it difficult to taking reliable data. The main difficulty is to achieve a constant magnetic field and impose them on sensors in certain angular positions. This occurs when the object that door sensors lacks symmetry to tipping or accommodation at certain angles.

One application of the Helmholtz coil described in this work will be to produce the constant fields at any angle within a certain volume, to provide the calibration of magnetic sensors embedded in equipment.

The Experience MEMS-VSB (Granziera Jr. *et al.*, 2011b)(Batista *et al.*, 2014) is one of the equipments which sensors will be calibrated using the coil. It carries multiple MEMS sensors, including several three-axis magnetometers. Its tetrahedral shape hinders tipping to measure the Earth's magnetic field. Then the Helmholtz coil will cancel the terrestrial field and generate field vectors in the directions needed for data acquisition to the best execution of the Triad estimation parameter algorithm (Granziera Jr *et al.*, 2011a).

Another use of the Helmholtz coil is on hardware-in-the-loop (HIL) simulations. With this type of coil it is possible to develop a system capable, for example, of simulating a geomagnetic model. Therefore it can be used to simulate the trajectory and attitude of a suborbital flight, which in this case is one of the possibilities to simulate the environment where MEMS-VSB experience will be used.

Though the theory behind the Helmholtz coil is relatively well known, the design and construction of a three-axial coil is not that trivial and commercial devices are quite expensive. This way, there are a lot of recent works aiming on the construction of three axis coils, such as the works of Carrara (2010), Oliveira *et al.* (2012) and Beravs *et al.* (2014). This work presents the design, requirements and details of the Helmholtz coil that was built as well as the mainly applications where it will be used.

Next section briefly presents the main aspects and requirements of the project, followed by the theoretical basis of Helmholtz theory. Next there is a the structural and electrical design chosen for the coil built. Finally it is presented both applications that the device was mainly built for. Last section discuss the results obtained from this project and also the advantages seen on the Helmholtz coil proposed in this work.

2. COIL DESIGN MAIN REQUIREMENTS

The first requirement for the Helmholtz coil design is that it must be capable of generating an uniform magnetic field in a cubic volume of approximately $11\ \mathrm{cm}$ edge. This region must ensure some uniformity between the center field and the extremes of up to 0.02% difference, being that the second requirement. For the cancellation of the Earth's magnetic field and subsequent generation of a new field in either direction the coil have to generate at least $1,2$ G in each axis. Thus, it was empirically established that the coil must be capable of generation a magnetic field of up to $2,0$ G per axis.

Aiming a greater ease on the construction and assembly it was chosen to build pairs of coils in square shape with rounded corners. While circular coils are better on the winding process, its manufacturing and the fixing structures between the pairs are far more complex, resulting in a higher cost and less design flexibility (Spencer and Davis, 1999). Square coils can be built simply through straight aluminum profiles and the uniform volume generated is suitable for testing equipments with rectangular shape.

3. THEORETICAL BASIS

To carry out the design of this system is necessary to predict the behavior of the generated magnetic field in the neighborhood of the coil's center. In order to simplify the analysis, the magnetic field is determined at the midpoint between the two windings and a uniform region that meets the design criteria will be found.

3.1 Mathematical Modeling

The magnetic field $\mathbf{B}$ at a given point A originated due to a current element $d\mathbf{l}$ (Fig. 1(a)) is obtained by Biot-Savart's law, which describes the magnetic field generated by an electric current i. This is described in Eq. 1.

$$d\mathbf{B}_A = \frac{\mu_0 i}{4\pi r^2} d\mathbf{l} \times \hat{\mathbf{r}} \tag{1}$$

This field is proportional to i, dl, $\sin\theta$, where θ is the angle between $d\mathbf{l}$ and $\hat{\mathbf{r}}$, decreases as r^{-2} and has direction and direction given by the cross product rule. At last $mu_0 = 4\,pi10^{-7}\ unitN/A^2$, which is the magnetic permeability of vacuum.

However, an electric current is always associated with a closed circuit so there is no reason to break it into multiple elements, except as an auxiliary step in the calculation. Therefore, it is performed the integration of the current elements along each side of the square coil and then summing the contribution of each.

Now, considering the grouping of straight wires from on side of the coil (Fig. 1(b)) on the length L, all current elements contribute A to $d\mathbf{B}_A$ in the same sense and direction, simply integrate $d\mathbf{B}_A$ from $-L/2$ to $+L/2$. The magnitude of the

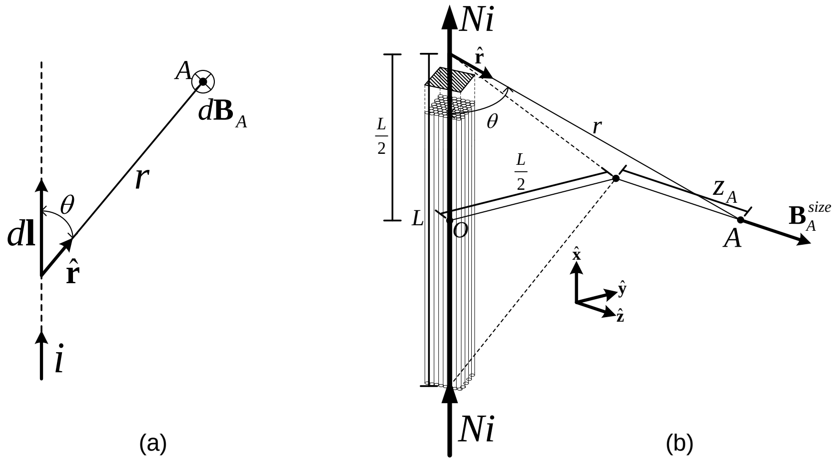

Figure 1. (a) Biot-Savart Law: magnetic field produced at the point A given a current i in a differential length dl at a distance r. (b) Field contribution generated in A by only one side of the coil.

produced field in A by the flow of current in one side of the coil is calculated by the Eq. 2.

$$B_A^{size}(z_A) = \frac{\mu_0 Ni}{4\pi}\frac{L}{2}\int_{-L/2}^{L/2}\frac{dx}{\left(z_A^2 + \left(\frac{L}{2}\right)^2 + x^2\right)^{3/2}}, \tag{2}$$

where N is the number of turns, i is the current in each wire and z_A is the distance from point A to the center of the coil. Also the relations on the Eq. 3 have been considered.

$$\sin\theta = \frac{L/2}{r}; \qquad r = \sqrt{x^2 + z_A^2 + (L/2)^2}; \tag{3}$$

Using the identity $\int \frac{dx}{(a^2+x^2)^{3/2}} = \frac{x}{a^2\sqrt{a^2+x^2}}$ it is obtained the contribution of one side of the coil side on the generated field at a distance z_A, given by Eq. 4.

$$B_A^{size}(z_A) = \frac{\mu_0 Ni}{\pi}\frac{L^2}{(4z_A^2 + L^2)\sqrt{4z_A^2 + 2L^2}} \tag{4}$$

Therefore, due to symmetry, the intensity of the field generated by a single pair of Helmholtz coil due to the distance z_A can be calculated by the summing of the contribution given by each of the four sides. Fig. 2) represents this idea while Eqs. 4 and 5 shows the total insensity.

$$B_O^{total}(z_A) = 4B_A^{size}(z_A) + 4B_A^{size}(-z_A) \tag{5}$$

$$B_O^{total}(z_A) = \frac{8\mu_0 NiL^2}{\pi(4z_A^2 + L^2)\sqrt{4z_A^2 + 2L^2}} \tag{6}$$

As z_A is equal to $\sigma L/2$, where σ must be found to maximize the uniformity of the field around the origin, the ultimate expression of the field produced by the Helmholtz coils at the origin O is given by Eq. 7.

$$\mathbf{B}_O^{total}(\sigma) = \frac{8\mu_0 Ni}{\pi L}\frac{1}{(\sigma^2 + 1)\sqrt{\sigma^2 + 2}}\hat{\mathbf{z}} \tag{7}$$

Eq. 7 defines the field intensity on the center point as a function of σ. This parameter σ is a constant that relates the distance between coils with the length L.

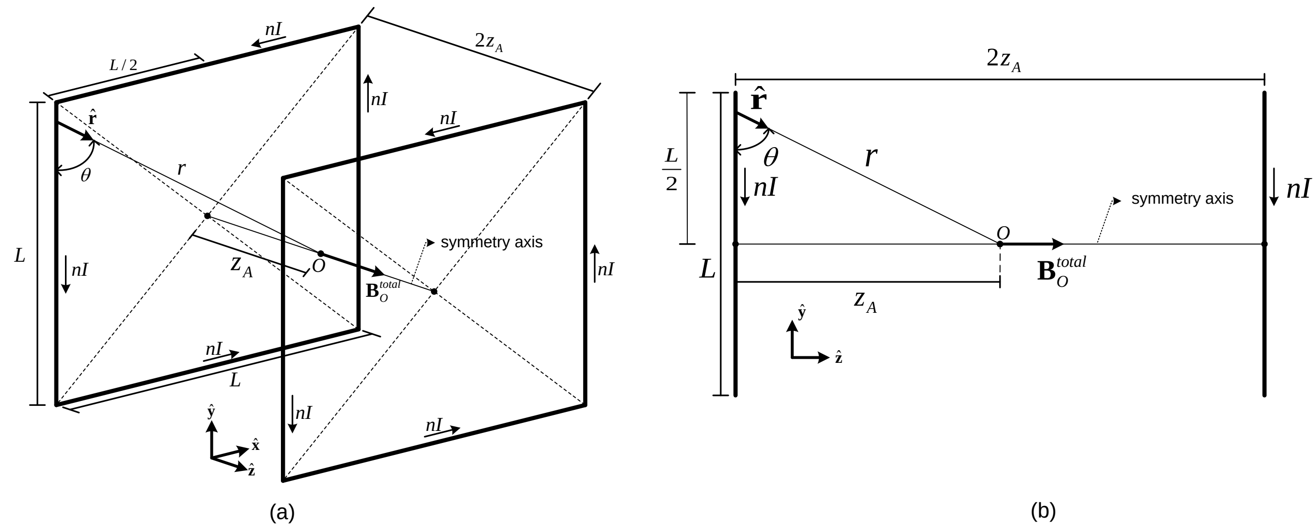

Figure 2. Representation of the magnetic field generated in O by the Helmholtz coils

3.2 Optimal Distance between the Coils

According to Spencer and Davis (1999) the maximization of the field uniformity around the origin point O is related with the distance (σL) between the coils. That is, there is an optimum distance where the variation of the field is minimized along the symmetry axis and close to the point O.

This analysis which aims on reducing the field variation implies zero how many derivatives are possible on Eq. 7. Due to system symmetry the first derivative (Eq. 8) will be zero only for $\sigma = 0$, which is not a valid distance.

$$\left.\frac{dB_O^{total}}{d\sigma}\right|_{\sigma=0} = \frac{8\mu_0 Ni}{\pi L}\left(\frac{-\sigma\left(3\sigma^2+5\right)}{(\sigma^2+1)^2(\sigma^2+2)^{3/2}}\right) = 0 \tag{8}$$

Though, the second derivative, given in Eq. 9, will be zero for any σ that resets the numerator. The polynomial $6\sigma^6 + 18\sigma^4 + 11\sigma^2 - 5$ has to real roots: $\pm 0,544505643$.

$$\frac{d^2B_O^{total}}{d\sigma^2} = \frac{8\mu_0 Ni}{\pi L}\left(\frac{2\left(6\sigma^6+18\sigma^4+11\sigma^2-5\right)}{(\sigma^2+1)^3(\sigma^2+2)^{5/2}}\right) = 0 \tag{9}$$

This way it is defined that the optimum distance between the coils is equal to $2z_A = \sigma L = 0,544505643L$.

To confirm that the σ found maximizes the uniformity around the point O, the third derivative must be greater than zero. The third derivative value for $\sigma = 0,544505643$ is shown on Eq. 10.

$$\left.\frac{d^3B_O^{total}}{d\sigma^3}\right|_{\sigma=0,544505643} \approx 2,908 \tag{10}$$

Since the optimum distance for the coils has been determined, Eq. 7 can be rewritten in the form of Eq. 11.

$$\left|\mathbf{B}_O^{total}\right| = 1,628733676 \cdot 10^{-6}\frac{Ni}{L}\ \mathrm{T}, \tag{11}$$

where the total field intensity, given in Tesla, is directly proportional to the number of turns N and to current i and inversely proportional to the length L.

3.3 Uniformity region

Through the mathematical model shown above it is possible to verify that the optimum coil distance is critical to maximize the field uniformity. Fig. 3 shows the difference of the field in relation to its value at point O given a shift in the axis of symmetry (Carrara, 2010).

As it is necessary to ensure σ's accuracy to meet the design requirement of $0,02\%$ field uniformity, through the graphic it is possible to identify that for $\sigma = 0.544505643$ the region within the requirement will have a length of $0,12591203L$.

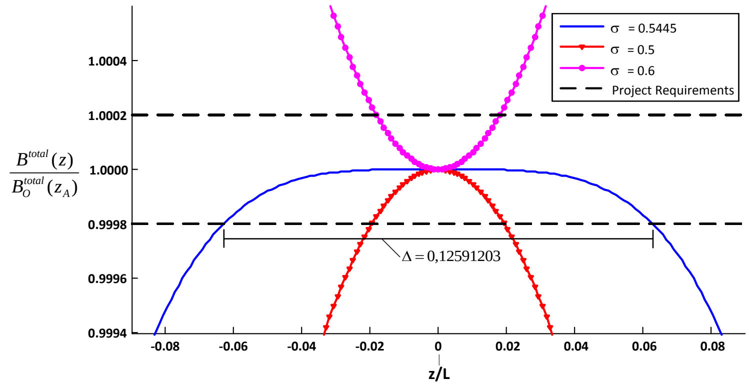

Figure 3. Field variation for different distances between the coils used to determine the uniformity of the region according to the design requirements.

4. HELMHOLTZ COIL DESIGN

In this coil set design both the structural and electrical parts are interconnected, meaning that any changes in the structural dimensions will implicate in a new group of values for parameters like number of turns, wire length on each coil, the cubic volume of uniformity around the origin among others. The same happens if there are changes in the electrical design. Though the electrical and structural projects are interconnected they are presented independently.

4.1 Structural Design

As mentioned, the rectangular coil was chosen so that aluminum profiles could be used as well as other commercial parts, avoiding manufacturing of expensive parts. Fig. 4a shows the chosen tubular aluminum profile (with 30 mm) to be the main structural part of the coil. This profile was selected due to its mechanical strength, symmetry and the presence of channels, which can facilitate not only the winding but also fixing others structural parts, such as plates and angle brackets.

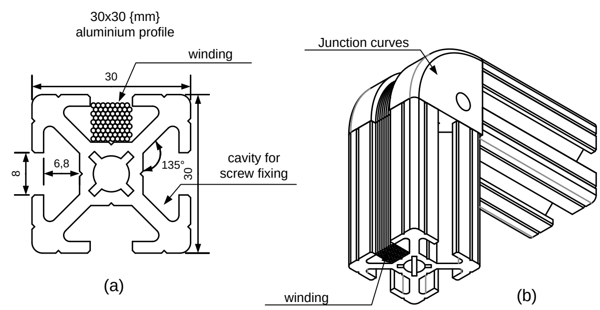

Figure 4. Main structural profile used on the coils with the junction accessory to facilitate wire winding.

Because it is a Helmholtz coil of three axes (3 pairs of coils), there is the innermost, the medium and the external pairs. These were designed so there would be no spaces between each pair.As the length L of the coils is related to the size of the uniform region that should be generated, the internal pair is obviously the one that produces the lowest region and its lengths is the most critical. Therefore, as the aforementioned relationship obtained from Fig. 3, the value of the internal pair will be given as the equation 12.

$$L_{Coil}^{int} = \frac{11,0}{0,12591203} \approx 88,0 \text{ cm} = 880 \text{ mm}, \tag{12}$$

where L_{Coil}^{int} is the average length of the pair of winding the innermost coil.

The coils size for the medium and the external (L_{Coil}^{mid}, L_{Coil}^{ext}) pairs can be found similarly to the profiles by simply adding 60 mm to the subsequent pair, since one profile has 30 mm of size.

Other auxiliary parts have been used and manufactured to improve the mechanical strength and the assembly accuracy of the coil. Fig. 4b illustrates the main accessory manufactured to be notched on the profiles junctions. This part has no structural function, but it is important on directing the wire to the next side of the square coil.

4.2 Electrical Design

All the electrical dimensioning of the project depends on the wire gauge choice. Selecting a particular wire gauge took into consideration the ease of the coiling process, the maximum number of turns within the useful area of the profile, the maximum electrical current, the resistance and length required for coiling all the coils.

Within several possibilities, wires gauges from 17 e 21 AWG are the ones that best fit the requirements. Wires under 17 AWG have a diameter inappropriate for coiling. Moreover, using of thinner wires would greatly increase the number of turns needed in each coil. Oppositely, thicker wires can not be molded into the coil form and in addition to it wires over 21 AWG might not withstand the tension needed for coiling. Through this empirical analysis the 19 AWG wire was chosen for the project. This choice is a compromise between facilitating the coiling process and a reduced number of turns per coil, withstanding the electrical current needed. Also, this wire supports a current of 2 A without overheating or losing its insulation capacity.

Eq. 11 is used in order to verify the number of turns needed in each of the coil pairs and also if that number does not exceeds N_{max}. In it, just isolate N and replace the remaining variables. For each of the pairs there is a minimum number of turns that will guarantee the necessary field intensity without exceeding the maximum current allowed in the wire. This number is presented on Tab. 1. With the number of turns, it is possible to calculate the others electrical parameters for the designed coil. It is important to emphasize that both coils for each pairs will be serially connected, to guarantee that the current will be the same. The same table shows all these others parameters. The maximum power showed on Tab. 1 was calculated for a single axis coil, so when serially connected the power needed will be twice as shown.

Table 1. Theoretical Electrical Parameters for the design Helmholtz Coil

Coil Type	N_{min}	**Coil Length (m)**	**Resist. (Ω)**	**Max Cur. (A)**	**Max Volt. (V)**	**Max Pwr (W)**
Inner	62	218.2	5.71	1.76	10.1	17.7
Medium	66	248.2	6.49	1.76	11.4	20.1
External	70	280.0	7.32	1.76	12.9	22.7

4.3 Helmholtz Coil Prototype Results

Tab. 2 shows all the parameters measured and calculated considering the prototype that was built. All parameters were as expected by the design. The greater number of turns was possible and recommended, since the number on the design was the minimum to obtain the necessary field without exceeding the maximum current. The resistance measured is almost the same for each axis of each pair, which shows that the coiling process was performed as expected.

Table 2. Electrical parameters obtained on the coil prototype

Coil Type	**N**	**Aprox. Coil Length (m)**	**Measured Resistance (Ω)**		**Max Current (A)**	**Max Voltage (V)**	**Max Power (W)**	**Inductance (mH)**	
			A	**B**				**A**	**B**
Inner	63	225.2	5.89	5.89	1.76	10.4	18.3	8.9	11.1
Medium	72	272.7	7.13	7.13	1.76	12.6	22.1	15.0	13.6
External	72	291.0	7.60	7.61	1.76	13.4	23.5	15.8	16.3

The comparison between the design and the prototype after its final assembly can be seen in Fig. 5. The manual assembly was easy and possible due to the commercial profiles used and its fixing components.

5. APPLICATIONS

One of the purposes of this Helmholtz coils project is to use it as an instrument for magnetic sensors calibration. Therefore it is necessary that the coil provides a constant magnetic field in predetermined directions controlled by a fed back field generation system.

This system, currently being implemented, is shown in Fig. 6. To generate the magnetic field, it was decided to use three current sources controlled by tension. Control voltages are provided by the DACs in one of the dSPACE hardware interface cards. To close the field control loop is used a magnetometer FGM3D/250 Sensys. The signals from the magnetometer are conditioned and sent the ADC inputs of the dSPACE hardware. The control algorithm which maintains the controlled field inside the coil in real time in the wheel after DSPACE be programmed via Simulink on a workstation connected to DSPACE through an optical interface. This workstation functions as a terminal type to control and view the dSPACE signals.

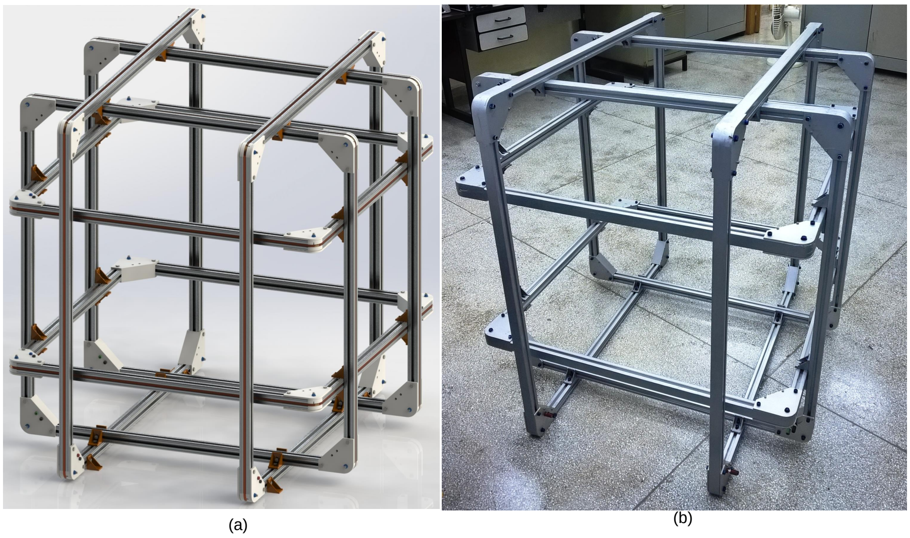

Figure 5. (a) Three-axis Helmholtz coil project. (b) Three-axis Helmholtz coil built

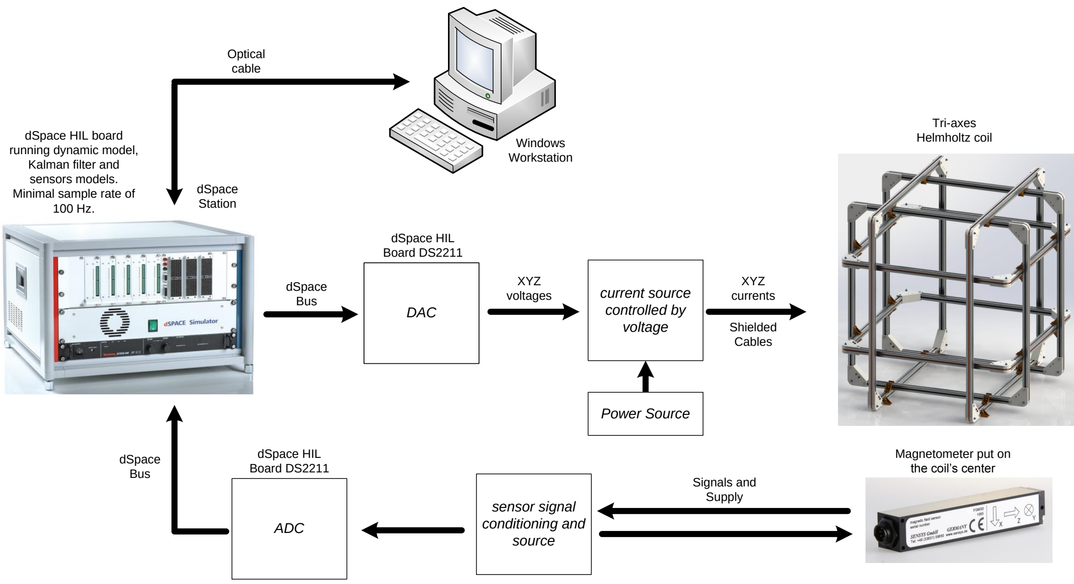

Figure 6. Control diagram of the Helmholtz coil

Once the coil is already generating static fields, the next step is to incorporate it as a hardware-in-the-Loop (HIL) simulation element and then making the field generated by the coil vary according to a kinematic attitude model.

The MEMS-VSB equipment will be the first tested by the coils, both for the calibration of magnetic sensors as to perform HIL simulations. In the HIL simulation, the trajectory and attitude of a suborbital flight will be simulated. The platform position and attitude calculated will provide inputs to geomagnetic model (such as WMM2015). The calculated field is generated and applied to the MEMS-VSB by the Helmholtz coils system. The simulation can also include other MEMS-VSB sensors, such as accelerometer and turns just by including the dynamic model of the vehicle. The sensor data are calculated by the model end passed directly to the equipment on board computer through dSPACE DAC board. The expected effects of HIL simulation are precisely subjecting the MEMS-VSB to the nearest possible condition of operation in flight. In this way both the operation of MEMS-VSB hardware and software is assured.

6. RESULTS AND CONCLUSIONS

In order to validate the built prototype, an initial setup using three independent Agilent current sources were first set to a point where the field obtained by the FGM3D/250 sensor was zero in all axis. After that, a 2 A current was applied only on the internal pair, creating a maximum field around the Z axis. After that the sensor was carefully moved around the other axis. Fig. 7 shows the result obtained.

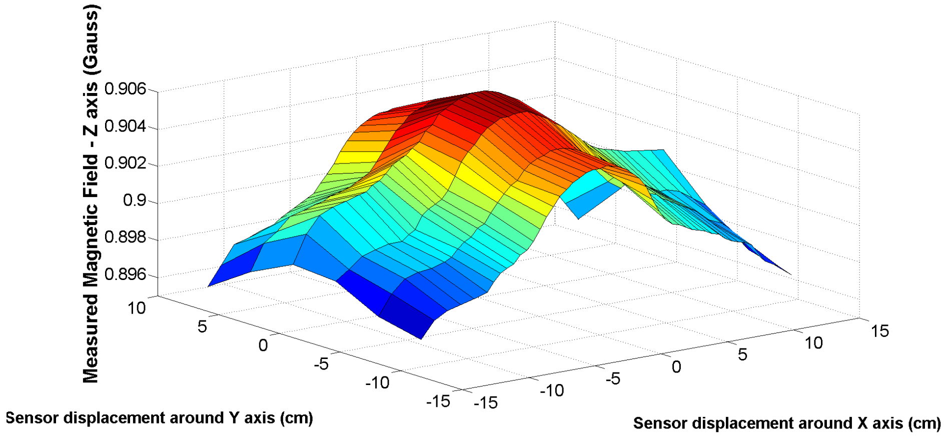

Figure 7. Measured Magnetic Field for a constant current applied only on a single axis after reseting field in all three axis.

The measurements showed that the worst variation was 0.6% considering the vertices formed by a $10\ \mathrm{cm}^2$ and the center of the coil.

Although not new the three axes Helmholtz coil design shown in this paper has presented some constructive innovations, making it possible to implement it in a very short time and with limited financial resources.

The calibration and HIL simulation setup described in this paper is almost complete and will enable the calibration of equipments with integrated magnetometers and also performing dynamic simulations with electromagnetic field variations.

The dSPACE hardware provides the capability to run dynamic systems in real time and simultaneously making the injection and reading of analog and digital signals to the equipment under test in order to simulate its hardware and software. In addition it is possible to monitor, record and control the run-time simulations through a workstation.

7. ACKNOWLEDGEMENTS

The authors thank the Brazilian Space Agency for the support through Uniespaço announcement and also the State University of Londrina for supporting the implementation of this project.

8. REFERENCES

Batista, D.S., Granziera Jr, F. and Tosin, M.C., 2014. “Sistema Mecatrônico baseado em Sensores MEMS voltado à Determinação de Atitude em Pequenos Satélites”. In *XX Congresso Brasileiro de Automática*.

Beravs, T., Begus, S., Podobnik, J. and Munih, M., 2014. “Magnetometer calibration using kalman filter covariance matrix for online estimation of magnetic field orientation”. *Instrumentation and Measurement, IEEE Transactions on*, Vol. PP, No. 99, pp. 1–1. ISSN 0018-9456. doi:10.1109/TIM.2014.2302240.

Carrara, V., 2010. “Projeto de bobinas de helmholtz em 3 eixos para simulação de campo geomagnético”. In *VI Congresso Nacional de Engenhria Mecânica*.

Foster, C.C. and Elkaim, G.H., 2008. “Extension of a two-step calibration methodology to include nonorthogonal sensor axes”. *Aerospace and Electronic Systems, IEEE Transactions on*, Vol. 44, No. 3, pp. 1070–1078. ISSN 0018-9251. doi:10.1109/TAES.2008.4655364.

Granziera Jr., F., Kuga, H. and Tosin, M.C., 2011b. “Attitude improvement and angular rate estimation using a Kalman filter with measurements of four tetrahedrally arranged low cost MEMS gyros”. In *X DINCON: Conferência Brasileira de Dinâmica, Controle e Aplicações*.

Granziera Jr, F., Vargas, R.H., Tosin, M.C. and Júnior, O.T., 2011a. “Self-calibration of mems sensors arranged in triads using kalman filter estimator”. In *COBEM*.

Oliveira, D.A., Carrara, V. and Kuga, H.K., 2012. “Calibração de bobina de helmholtz para aplicação espacial utilizando filtragem com mínimos quadrados”. In *Guidelines of 3o Workshop on Space Engineering and Technology*.

Spencer, J.D. and Davis, R.H., 1999. “Helmholtz coils for mil-std-462d rs101 testing”. In *Electromagnetic Compatibility*. Vol. 2, pp. 940–942.

9. RESPONSIBILITY NOTICE

The authors are the only responsible for the printed material included in this paper.